

PAPER • OPEN ACCESS

An algorithm for automated lattice design of transfer lines

To cite this article: S Reimann *et al* 2019 *J. Phys.: Conf. Ser.* **1350** 012110

View the [article online](#) for updates and enhancements.

You may also like

- [Comparative analysis on flexibility requirements of typical Cryogenic Transfer lines](#)
Mohit Jadon, Uday Kumar, Ketan Choukekar et al.
- [The FAIR Heavy Ion Synchrotron SIS100](#)
P. Spiller, R. Balss, P. Bartolome et al.
- [Hydraulic adjustment of the two-phase helium forced flow cooled superconducting magnets of the SIS100 heavy ion synchrotron for FAIR](#)
A. Bleile, V. Datskov, E. Fischer et al.



The Electrochemical Society
Advancing solid state & electrochemical science & technology

242nd ECS Meeting

Oct 9 – 13, 2022 • Atlanta, GA, US

Abstract submission deadline: **April 8, 2022**

Connect. Engage. Champion. Empower. Accelerate.

MOVE SCIENCE FORWARD



Submit your abstract



An algorithm for automated lattice design of transfer lines

S Reimann^{1,2}, M Droba¹, O Meusel¹ and H Podlech¹

¹ IAP, Goethe University, Frankfurt am Main, Germany

² GSI Helmholtz Centre, Darmstadt, Germany

E-mail: s.reimann@gsi.de

Abstract. Since the last 20 years, modern heuristic algorithms and machine learning have been increasingly used for several purposes in accelerator technology and physics. Since computing power has become less and less of a limiting factor, these tools have become part of the physicist community's standard toolkit [1][2] [3] [4] [5]. This paper describes the construction of an algorithm that can be used to generate an optimised lattice design for transfer lines under the consideration of restrictions that usually limit design options in reality. The developed algorithm has been applied to the existing SIS18 to HADES transfer line in GSI.

1. Introduction

Beside the necessary instrumentation, transfer lines usually consist of quadrupoles, dipoles, steerer magnets and buncher cavities. Sometimes the dipole positions are more or less fixed and therefore boundary conditions for the optimisation. For showing the idea, assumed that the geometry of the transfer line is given, which means that the number and position of the dipole magnets, as well as the start and end point. The goal is, to place 2 types of quadrupoles in between the dipoles such that a given particle distribution will be guided through the beam line with maximal transmission and focused on a target. The algorithm has been designed in such a way that minimizes both the power consumption and the required number of components.

2. Genotype parameterisation

Without limiting the generality we assume to have in stock 2 standard quadrupoles Q_a and Q_b with associated lengths L_a and L_b , where $L_b > L_a$. Another assumption is, that each quadrupole type is used for a different area of values for the normalized integrated field gradient $kl = B'l/(B\rho)$. These areas are distinct and do not overlap.

$$\text{area 1: } (kl)_0 < |kl| \leq (kl)_a$$

$$\text{area 2: } (kl)_a < |kl| \leq (kl)_b$$

The simplest transfer line is a straight line and contains no further elements. Such a transfer line of a given length L can be divided in n sections of equal length. If we consider the solution with maximal number of the longest quadrupoles Q_b , in general the number n can not be bigger than L/L_b . In order to accommodate free space between the quadrupoles, one quadrupole is left out. Therefore the number of sections is



$$n = \frac{L}{L_b} - 1$$

In order to be able to use a metaheuristic optimization method such as a genetic algorithm [6], it is necessary to find a suitable parameterization for the corresponding problem. The parameters (an array of real numbers) are called the genes. For this work, the number of genes within a genome G is $2n$. Even genes ν_i represent the kl value of quadrupoles and odd genes μ_i represent the relative distance between the quadrupoles. All genes are real numbers.

$$G = \{\mu_1, \nu_1, \mu_2, \nu_2, \dots, \mu_n, \nu_n\}$$

3. Phenotype construction

The phenotype of the genome G is then constructed in the following way. For all ν_i , the constructed element E_i is either one of the standard quadrupoles or a drift line D , depending on the value of ν_i . For quadrupoles, ν_i is an expression of the kl value.

$$\begin{aligned} 0 < |\nu_i| \leq (kl)_0 &\implies E_i = D \\ (kl)_0 < |\nu_i| \leq (kl)_a &\implies E_i = Q_a \\ (kl)_a < |\nu_i| \leq (kl)_b &\implies E_i = Q_b \end{aligned}$$

In this manner it can be assured, that a quadrupole with more focusing power is used only, if more focusing power is really needed. The length of the constructed quadrupole (l_i) is defined by its type ($E_i = Q_a \implies l_i = L_a$, $E_i = Q_b \implies l_i = L_b$) and its strength can be calculated from

$$k_i = \frac{\nu_i}{l_i}$$

A discontinuity at the transition from Q_a to Q_b type quadrupoles can not be avoided, if both types have different lengths. The continuity can only be conserved for the kl value (Figs. 1, 2).

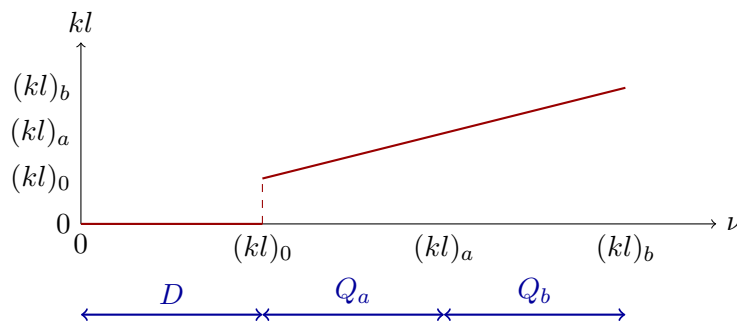


Figure 1. dependence of kl on ν value.

In cases where the focusing power is lower than the threshold $(kl)_0$, a zero field quadrupole (drift line) D is used. The length of this drift line is set to

$$l_i = \frac{|\nu_i|}{(kl)_0} L_a$$

A continuity in length can be created in this way, but a jump for kl is unavoidable, between drift and quadrupole elements. A smooth transition of kl to zero, would create quadrupoles for

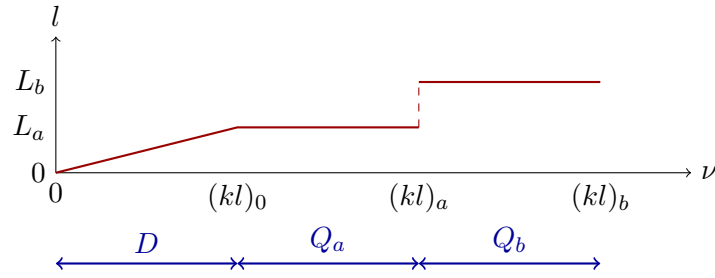


Figure 2. dependence of length l on ν value.

even smallest kl values and all transfer lines would end up full of quadrupoles. So the resulting strength k of the created element has by default two discontinuities (Fig. 3).

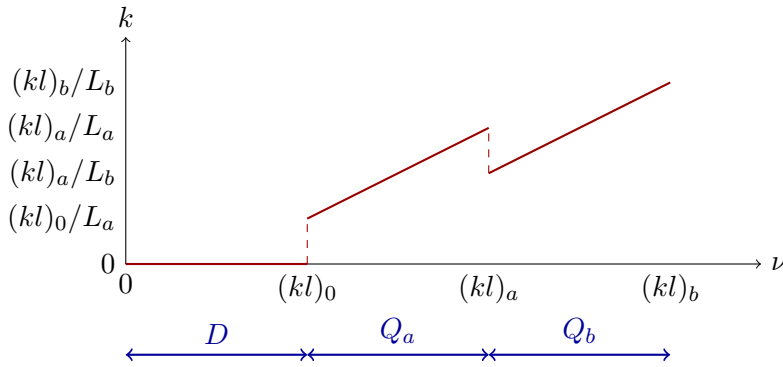


Figure 3. dependence of quadrupole strength k on ν value.

Table 1 contains the properties of the standard quadrupole types as they can be extracted from the genome.

Table 1. standard elements E_i (quadrupoles and drift).

E_i	condition	length l_i	strength k_i
D	$0 < \nu_i \leq (kl)_0$	$\frac{\nu_i}{(kl)_0} L_a$	0
Q_a	$(kl)_0 < \nu_i \leq (kl)_a$	L_a	$\frac{\nu_i}{L_a}$
Q_b	$(kl)_a < \nu_i \leq (kl)_b$	L_b	$\frac{\nu_i}{L_b}$

Once the standard quadrupoles are constructed, the distances between the elements (and therefore their positions) are calculated. The remaining space is

$$L_r = L - \sum_{i=1}^n l_i$$

and the distances between the elements are proportional to the share of μ_i .

$$d_i = \frac{\mu_i}{\sum_{i=1}^n \mu_i} L_r$$

4. Evaluation function

A given genotype is tested with regards to its fitness. Therefore the phenotype or rather the lattice of the transfer line is constructed for each genome. If the solution should match a given acceptance by the user, an additional aperture is appended. Subsequently m particles with a given distribution are tracked through each solution via matrix multiplication¹ and the following indicators are collected.

L_p	...	the flight distance for each particle
T	...	the overall transmission (N_{end}/N_{init})
N_q	...	the resulting number of quadrupoles
$\Sigma_{ kl }$...	the sum of absolute value of strengths

The evaluation function for each genome $F(G)$ is the weighted sum of all indicators normalised to 1. The weights ω_i can be chosen according to the priorities of the different indicators.

$$\begin{aligned} F(G) = & \omega_1 \cdot (1 - (1/m) \cdot \Sigma_p(L_p/L)) \\ & + \omega_2 \cdot (1 - T) \\ & + \omega_3 \cdot N_q/n \\ & + \omega_4 \cdot \Sigma_{|kl|}/(n \cdot (kl)_b) \end{aligned}$$

A simple genetic algorithm has now been used to minimise F . Any other algorithm that avoids local minima (such as particle swarm algorithm [7] or BOBYQA [8]) could be used as well.

5. Results

The developed algorithm has been tested against theoretical cases (trivial, doublet and target focusing) and a realistic one. The latter concerns the transfer line between SIS18 and HADES [9] at GSI. In all of them space charge is not considered and the weights have been set to $\omega_1 = 1$, $\omega_2 = 1$, $\omega_3 = 0.01$ and $\omega_4 = 0.0001$. A common circular vacuum chamber of 0.12 m diameter is assumed throughout the entire transfer line. The particle distribution contains 1000 particles entering on-axis and features a Gaussian shape in all 5-coordinates x , x' , y , y' and $\Delta p/p$ (see Table 2).

Table 2. Characteristic dimensions of the standard particle distribution of SIS 18 (slow extraction parameters from synchrotron SIS18 @ GSI [10]).

dimension	1-sigma	dimension	1-sigma
x	2.941 mm	y	3.531 mm
x'	0.353 mrad	y'	0.567 mrad
$\Delta p/p$	0.001		

The genetic algorithm uses 200 individuals (genomes) per generation, therefore 200000 particles have to be tracked in each optimisation step.

¹ drift and quadrupole elements are represented by a 5x5 matrices Ref. [11]

5.1. Trivial solution

In case of no additional aperture limitations besides the vacuum chamber, one can estimate the length of the transfer line where the beam (with the given particle distribution) goes through without losses.

$$y_{max} = 0.06 \text{ m} > 3\sigma_y + 3\sigma_{y'}L \implies 29.0 \text{ m} > L$$

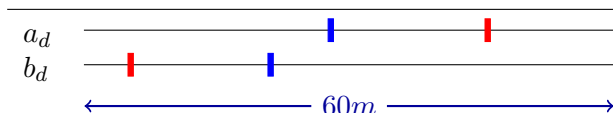
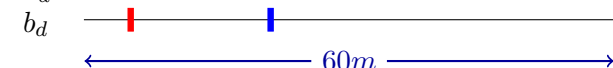
So, for a distance of $L = 25 \text{ m}$, the beam could be transported without additional focusing (assuming the σ_y and $\sigma_{y'}$ given in Table 2). The optimisation has been executed 20 times and in all cases, the algorithm found the optimal solution within less than 30 generations.

5.2. Doublet solution

The next example is a 60 m transfer line, where a 100 % Transmission is not possible without additional focusing and hence there is no solution without quadrupoles.

Table 3 shows the 2 found solutions a_d and b_d . In any case the solution is a quadrupole doublet, in 70 % of the solutions the doublet starts using a vertical focusing (blue) and in 30 % with a horizontal focusing (red) quadrupole. The needed quadrupole strength for solution a_d is slightly lower than solution b_d .

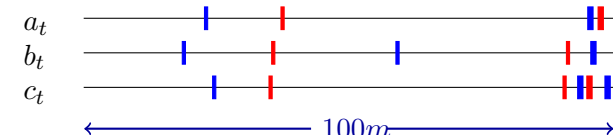
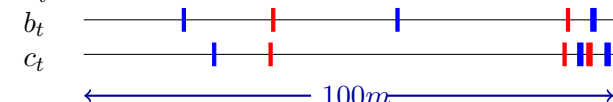
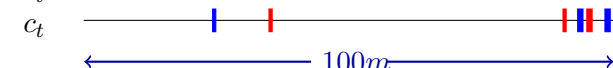
Table 3. lattice solutions for the 60 m case.

#	lattice
a_d	
b_d	

5.3. Target focusing

Next considered case is a 100 m transfer line with a target circular aperture limitation of 5 mm (diameter) at the end of it. 3 solutions have been found (a_t , b_t and c_t) with 100 % transmission (see Table 4). The prevalence of solutions can be suppressed by varying the weights ω_j .

Table 4. lattices for 100 m transfer line with final aperture limitation.

#	lattice
a_t	
b_t	
c_t	

5.4. Transfer line SIS18 to HADES experiment

Our last case of study concerns the 160 m long transfer line that transports the beam from the SIS18 synchrotron to the HADES experiment. This transfer line is presently under review [9], as well as all the existing GSI transfer lines [12], due to need for improving the transmission when

running at high intensity [13]. The algorithm assumes a 5 cm long target with 2.2 mm diameter [14] at the end of the transfer line. The result obtained with 100 % transmission and smallest F is shown in Table 5 (b) against the present transfer line (a).

Table 5. both HADES lattices (length ca. 160 m), the existing version (a) and the solution from the algorithm (b), cyan elements are bending dipoles.

#	lattice
a	
b	

The result looks quite different to the existing version. The strength of element number (14 vs. 20) is much lower and the strong quadrupole (Q_b) is only used twice. Since intermediate foci are not excluded by the algorithm, they are part of the solution (Fig. 4). This beam line is also used for other purposes (the dipoles (cyan) distribute the beam also to other target stations) and for fast extraction, where the horizontal emittance is higher by a factor of 6, so some margin for deviations should be foreseen. This could easily be added to the algorithm by artificially limiting the aperture. At the moment the full aperture is used at some positions.

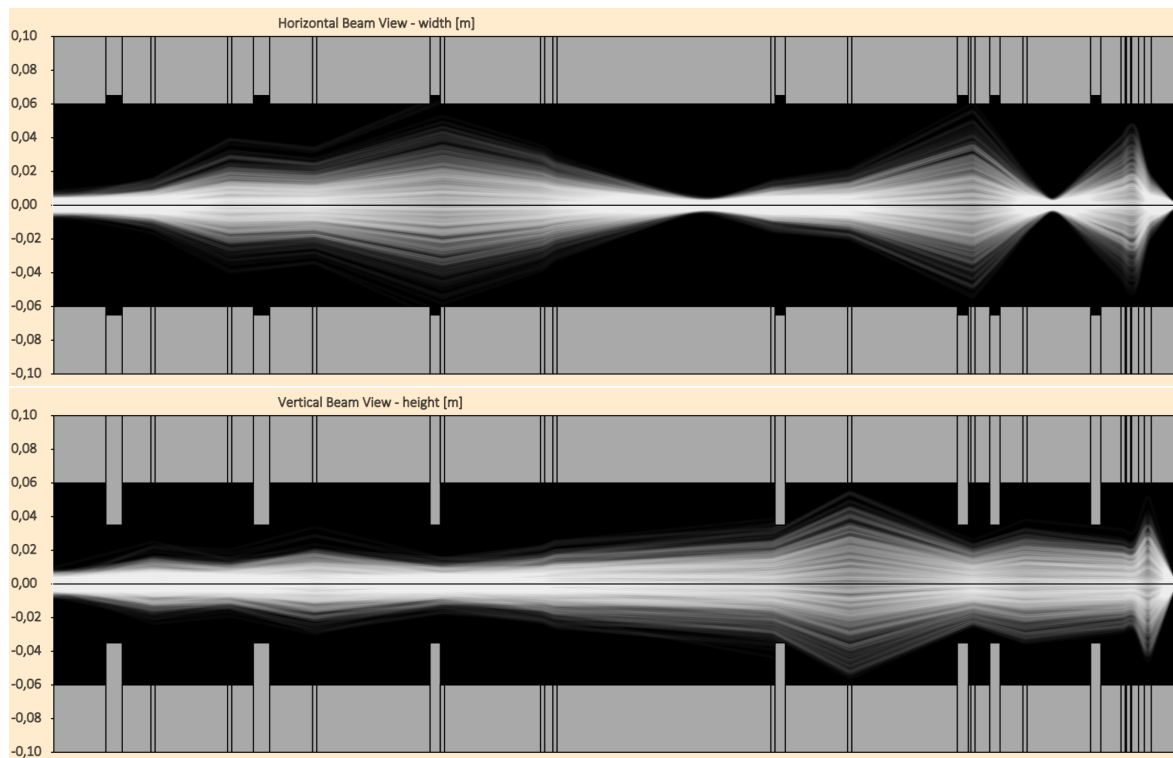


Figure 4. HADES lattice and optics, found by the algorithm, top = horizontal beam size, bottom = vertical beam size.

6. Conclusion

In all the considered transfer lines, the algorithm has found optimal solutions in terms of transmission while minimising energy consumption and number of elements. The algorithm will be further developed and investigated. Additional elements as buncher cavities are about to be included as well as high current effects. Next step is the comparison with experiments and existing solutions. All transfer lines of GSI/FAIR [15] will be reviewed and future lines could even be designed by the use of this algorithm.

References

- [1] Noll D, Chau L P, Droba M, Meusel O, Podlech H, Ratzinger U and Wiesner C 2011 *Proc. 2nd Int. Particle Accelerator Conf. (San Sebastian)* pp. 667–9
- [2] Streichert M *et al.* 2012 *Proc. 11th Int. Computational Accelerator Physics Conf. (Rostock-Warnemunde)* pp. 72–4
- [3] Appel S and Boine-Frankenheim O 2015 *Proc. 6th Int. Particle Accelerator Conf. (Richmond)* pp. 3689–92
- [4] Geithner W, Andelkovic Z, Appel S, Geithner O, Herfurth F, Reimann S and Vorobyev G 2018 *Proc. 9th Int. Particle Accelerator Conf. (Vancouver)* pp. 4712–5
- [5] Bakkali Taheri F, Apollonio M, Martin I P S, Bartolini R and Li J 2019 *Proc. 10th Int. Particle Accelerator Conf. (Melbourne)* preprint THPGW071
- [6] Mitchell M 1996 *An Introduction to Genetic Algorithms* (Cambridge: MIT Press Cambridge)
- [7] Kennedy J and Eberhart R 1995 *Proceedings of IEEE International Conference on Neural Networks* pp. 1942–8
- [8] Powell M J D 2009 *The BOBYQA algorithm for bound constrained optimization without derivatives* (Department of Applied Mathematics and Theoretical Physics, Cambridge University. DAMTP 2009/NA06)
- [9] The HADES Collaboration 2009 *Eur. Phys. J.* **A41** 243-77
- [10] Appel S 2019 (Darmstadt: GSI private Communication)
- [11] Hinterberger F 2008 *Physik der Teilchenbeschleuniger und Ionenoptik* (Berlin: Springer)
- [12] Sapinski M, Geithner O, Reimann S, Schuett P, Vossberg M and Walasek-Hoehne B 2019 *Proc. 10th Int. Particle Accelerator Conf. (Melbourne)* preprint MOPGW024
- [13] Sapinski M *et al.* 2017 *Proc. 8th Int. Particle Accelerator Conf. (Copenhagen)* pp. 2214–6
- [14] Pietraszko J 2016 *Slow extraction, input from HADES at SIS18* (Darmstadt: HIC4FAIR Workshop 2016)
- [15] Spiller P J *et al.* 2018 *Proc. 9th Int. Particle Accelerator Conf. (Vancouver)* pp. 63–8